Nuclear Morphometry and Molecular Biomarkers of Actinic Keratosis, Sun-Damaged, and Nonexposed Skin

Philip M. Carpenter,[1,2] Kenneth G. Linden,[1,3] Christine E. McLaren,[1,4] Kuo-Tung Li,[1] Shehla Arain,[2] Ronald J. Barr,[3] Pamela Hite,[3] Joannie D. Sun,[3] and Frank L. Meyskens, Jr.[1,5]

[1]The Chao Family Comprehensive Cancer Center; Departments of [2]Pathology and [3]Dermatology; and Divisions of [4]Epidemiology and [5]Hematology-Oncology of the Department of Medicine, the University of California Irvine, Irvine, California

Abstract

Computer-assisted image analysis is useful for quantifying the histologic and molecular changes of sun-induced squamous cell carcinoma progression. We used the CAS 200 image analysis system to measure nuclear morphometric parameters, p53 expression, and proliferation markers in actinic keratosis (AK), sun-exposed, and normal skin in 51 patients. Nuclear morphometry revealed significant increases in nuclear absorbance, irregularity of nuclear shape, and nuclear size in AK compared with normal and sun-damaged skin. These parameters showed significantly greater variability in AK nuclei. Argyrophyllic nucleolar organizer area and number were also significantly greater in AK compared with sun-damaged skin and normal skin. Ki67 and p53 expressions were both increased in sun-damaged skin relative to normal and greater still in AK. These data are evidence that sun damage induces proliferation and p53 abnormalities before the appearance of nuclear abnormalities and their associated DNA instability. Following these changes during a skin cancer chemopreventative trial can then help assess the efficacy of the agent and help determine where in the progression of neoplastic changes it exerts its biological effects. (Cancer Epidemiol Biomarkers Prev 2004;13(12):1996–2002)

Introduction

The development of squamous cell carcinoma (SCC) of the skin as a result of sun exposure is characterized by a progression of clinical (1), histologic (1, 2), and molecular (3, 4) changes. Sun-damaged skin may exhibit dermal solar elastosis and nuclear crowding, but only minor nuclear abnormalities or epidermal thickening. As sun damage progresses to actinic keratosis (AK), scaly erythematous plaques appear, with histologic features including epidermal thickening, dysplastic nuclei, and superficial parakeratosis. Dysplasia involving all layers of the epidermis defines carcinoma *in situ*, or Bowen's disease, which in turn may be followed by basement membrane invasion by tumor cells, the hallmark of SCC (2). Similarly, a series of molecular changes is observed in the progression of SCC (3, 5-9). One of the best-studied molecular markers is p53, a tumor suppressor (10, 11) that regulates apoptosis, cellular proliferation (5, 6, 12), and the response of skin to solar damage (13-25).

Because AK is a premalignant lesion (26), it is a target for prevention of SCC (19, 20, 27-29). Furthermore, reduction of the number of AK may be a marker of the efficacy of a prevention agent (28, 29). In a chemotherapeutic trial, it may also be useful to determine whether molecular morphologic changes occur early or late in the neoplastic progression of a lesion, which in turn could be helpful in determining where the agent interrupts the neoplastic cycle. Some of the surrogate biomarkers of SCC progression have included p53 mutation and immunohistochemical expression analysis, proliferation index, and apoptotic index (19, 29). Because nuclear abnormalities are a well-established finding in AK, these are potentially also a suitable biomarker for the evaluation of skin cancer prevention agents. For comparisons between treatments and placebo-controlled groups in chemoprevention and other trials, it is preferable to use quantitative measurements of biomarkers (30). Computer-assisted nuclear morphometric analyses have been used to obtain such measurements for a number of tumor types (30-33), but there have been only a few nuclear morphometric studies on cutaneous SCC and its precursors (34-39).

This report describes the nuclear morphometric parameters of AK compared with sun-exposed and normal skin in 51 patients. Computer-assisted quantitation of p53 immunohistochemistry and two proliferation markers were also done on the same lesions. The data indicate that the progression of normal to sun-damaged skin to AK was accompanied by increasingly abnormal values of nuclear DNA content, size, shape and variability, as well as increases in p53 expression, Ki67 labeling index, and nucleolar organizer size and number. Increased proliferation and p53 abnormalities preceded nuclear morphometric alterations in the progression of sun damage toward AK.

Received 2/23/04; revised 5/10/04; accepted 6/14/04.

Grant support: National Cancer Institute grants NO1-CN-85182-MAO and CA 62203.

The costs of publication of this article were defrayed in part by the payment of page charges. This article must therefore be hereby marked advertisement in accordance with 18 U.S.C. Section 1734 solely to indicate this fact.

Note: Morphometric measurements were done at the UCI Chao Family Comprehensive Cancer Center Translational Pathology Core Facility.

Requests for reprints: Philip M. Carpenter, Department of Pathology, Irvine Medical Center, University of California, Building 10, Route 40, Room 104, 101 The City Drive South, Orange, CA 92868, USA. Phone: 714-456-6141; Fax: 714-456-5873. E-mail: pmcarpen@uci.edu

Materials and Methods

Subjects. Patients with a history of chronic sun exposure were examined for clinical features of AK on sun-exposed surfaces of the upper extremities. These patients were recruited for a chemoprevention study of polyphenon E (epigallocatechin gallate). The clinical findings have been reported elsewhere in detail (40), but overall a difference in the regression rate of AK was not shown. A power analysis indicated that at least 50 patients were needed to assess the efficacy of the agent; thus, a total of 51 patients were enrolled, and their baseline biopsies provided the samples for analysis presented here. All patients had scaly, erythematous lesions clinically suspicious for AK bilaterally. Under local anesthetic, a shave biopsy each of probable AK and nearby sun-exposed but non-AK skin was done on both arms of each patient, resulting in a total of 102 AK biopsies and 102 sun-damaged skin biopsies. The sun-exposed area was taken from an area that had approximately the same degree of sun exposure as the AK. An additional 32 biopsies from skin protected from sun exposure were taken from 12 patients. The tissue was immediately fixed in 10% neutral buffered formalin, processed for paraffin embedding, sectioned, H&E stained, and examined by an experienced dermatopathologist (R.J.B.).

Biopsies were categorized by histopathology as normal, sun-damaged, or AK. Lesions interpreted as AK exhibited the following features: (1) focal atypical parakeratosis of the stratum corneum, often alternating with relatively normal stratum corneum overlying hair follicles and eccrine sweat ducts; (2) replacement of the lower 1/3 to 1/4 of the subjacent epidermis by cytologically atypical keratinocytes exhibiting considerable variation in nuclear size, shape, and staining characteristics; (3) an accompanying loss of normal maturation; (4) an increase in mitotic figures; (5) prominent solar elastosis of the dermis; and (6) often an associated inflammatory infiltrate composed of lymphocytes, histiocytes, and variable numbers of plasma cells. Lesions interpreted as sun-damaged skin exhibited the following features: (1) atrophy with flattening of the epidermal rete ridges; (2) a variable amount of epidermal melanosis; (3) minimal cytologic atypia of keratinocytes, if confined to scattered individual cells; (4) prominent dermal solar elastosis; and (5) minimal inflammation. A few biopsies were from areas clinically suspicious of AK, but showed SCC, or did not meet the histologic criteria for AK listed above. These cases were too few in number for meaningful analysis, and thus were excluded from our study. The Human Subjects Committee of the University of California, Irvine, approved this study.

Immunohistochemistry and Histochemical Staining. For each biopsy, 4-μm-thick sections were placed on capillary gap slides and deparaffinized with Histoclear (National Diagnostics, Atlanta, GA). Sections were then rehydrated through decreasing concentrations of isopropyl alcohol. Sections for immunoperoxidase staining were steam pretreated for 20 minutes in Antigen Retrieval Citra Buffer (Biogenex, San Ramon, CA). Avidin-biotin complex immunoperoxidase reactions were done using an Immunotech 500 automated immunostainer (Ventana Systems, Inc., Tucson AZ) according to the manufacturer's instructions. Briefly, the automated steps included blockage of endogenous peroxidase with 3% hydrogen peroxide and reaction with monoclonal antibodies against human p53 (clone D07, Dako, Carpinteria, CA) diluted 1:200, or Ki67 (clone MIB-1, Dako) diluted 1:100. The reaction was followed by a biotinylated goat anti-mouse IgG secondary antibody and then an avidin-biotin peroxidase complex. The chromogen was diaminobenzadine for all reactions. Cells were counterstained by 0.4% methyl green in 0.1 mol/L sodium acetate buffer (pH 4.0) followed by three washes each of water, 1-butanol, and Histoclear. Negative controls were done in the same fashion, except that the primary antibody was substituted with mouse immunoglobulin. A section of SCC provided the positive controls for p53 and Ki-67.

One section from each biopsy was stained with the Feulgen DNA Stain Kit (TriPath, Burlington, NC) according to the manufacturer's instructions.

Staining of argyrophyllic nucleolar organizers (AgNOr) was done by mixing 2 volumes of 50% silver nitrate with one volume of 2% gelatin and 1% formic acid, followed by immediate incubation of the slides in this mixture for 30 minutes (41). After rehydration in distilled water, the slides received a methyl green counterstain as described above.

Image Analysis. Image analysis was done on each section of 102 AKs, 102 sun-damaged areas, and 32 normal skin biopsies stained as described above, using the CAS 200 Image Analysis System (Becton Dickinson, San Jose CA). The theory and operation of the CAS system has been previously reported (42). A minimum of 200 epidermal cells were analyzed on each slide by an operator who had no prior knowledge of the clinical or histopathologic diagnosis of the biopsy specimen. Only cells with complete nuclear cross sections and no evidence of overlapping, parakeratosis, or apoptosis were analyzed.

On Feulgen-stained sections, the Quantitative DNA Analysis program was used to determine the average and SD of absorbance, nuclear shape, and nuclear size of the cells of each section. The operation of the Quantitative DNA Analysis program of the CAS 200 was done according to the manufacturer's instructions. Briefly, under optimized light settings, representative fields of cells were chosen by the operator, and threshold settings of the machine were chosen such that the program could identify individual nuclei with sizes and contours that matched as closely as possible to those seen under the microscope by the operator. The operator was able to reject cells which did not meet the criteria stated above and was able to instruct the machine to separately identify touching but nonoverlapping cells. Before analyzing cells, Feulgen-stained tetraploid rat hepatocyte nuclei were used to calibrate the absorbance readings.

Nuclear absorbance of Fuelgen-stained sections is expressed in arbitrary units, but the values are directly proportional to the DNA content of a single nucleus. Nuclear shape is expressed in arbitrary units, which increase as the outline of the cell deviates from a perfect circle. Thus, an irregularly shaped cell will have a higher value than one with a smooth outline. Nuclear size is expressed as the area of the nuclear cross section in μm^2. An in-depth description of these values and the algorithms that define them has been previously described (42).

In addition to these values, the variability of each of the three parameters (i.e., absorbance, shape, and size) was calculated. Variability was calculated by taking the SD of the readings of the nuclei within an individual biopsy. In specimens where there are greater variations between individual cells in a given parameter being measured, the SD will be greater for that parameter in that particular specimen. For this reason, the SD of a parameter serves as a measurement of variability or pleomorphism for that particular parameter.

Image analysis of sections stained by immunohistochemistry was done using the Quantitative Proliferation Index Program of the CAS 200, according to the manufacturer's instructions. Briefly, the operator chose thresholds at a wavelength of 620 nm for nuclei exhibiting methyl green counterstaining for identification by the machine as a cell nucleus and a separate threshold at 500 nm for the program to identify a nucleus as having a positive immunohistochemical reaction. This was done because the green counterstain is transparent at 500 nm; thus, only nuclei with a positive immunoperoxidase reaction will be detected by the instrument. The analysis was displayed as the percentage of positively staining cells.

Image analysis of silver-stained sections was done using the AgNOr Program, according to the manufacturer's instructions. Briefly, thresholds for total green-colored nuclei were chosen as described above, and thresholds for the darkly staining nucleolar organizers were chosen separately. The values were expressed as average AgNOr number per nucleus and average AgNOr area per nucleus.

To ensure accuracy of all of the computer-derived values, each slide was reviewed by a surgical pathologist (P.M.C.) who had no knowledge of the location of the biopsy or clinical diagnosis for each of the samples. Each value was estimated by visualization, and the estimates were compared with the computer-derived value. For apparent discrepancies, the section was either restained, reanalyzed with the computer or both.

Statistical Considerations. Quantitative biomarkers included measures of nuclear morphometry, proliferation, and p53. By the study design, two biopsies were taken from both arms of each patient. For statistical analysis, biopsy samples were treated as independent specimens. The average and SD of observed values were calculated for each of the 10 biomarkers and are reported in Table 1. For statistical comparison of groups, because the distributions of outcome measures were right skewed, transformations to induce normality were examined using the Box-Cox method (43). Based on this analysis, the square root transformation was applied to all outcome values. The significance of the differences between measurements of unexposed versus sun damaged, unexposed versus AK and sun-damaged versus AK was calculated, with three comparisons of means made for each of 10 biomarkers. To adjust for the multiple testing of several end points of comparable importance, the stepdown bootstrap resampling method was used and adjusted *P* values were computed (44).

Results

Patient Population. A total of 51 patients met the criteria of having biopsy proven AK in both arms and a biopsy showing sun-damaged skin from each arm. The patients included 42 males and 9 females. The age range was 44 to 86 years, with a median age of 63 years. One patient was black, and 50 patients were white.

Nuclear Morphometric Parameters. Nuclear morphometric values of Feulgen-stained epidermis derived using the CAS 200 image analysis system are summarized in the first three rows of Table 1. Skin protected from sun exposure showed epidermis with normochromatic, oval and small nuclei (Fig. 1A), reflecting the relatively low values for nuclear absorbance, shape, and size. Sun-damaged skin showed epidermal nuclei which were minimally or somewhat darker, more irregular, and larger than those of normal skin (Fig. 1B) with slightly greater values of the corresponding morphometric parameters, but the differences were not significantly different. In contrast, AK showed more prominent hyperchromasia, nuclear irregularity and greater nuclear sizes than the sun-damaged and normal cells (Fig. 1C). As expected, the nuclear measurements were significantly greater by image analysis.

Normal cells in most tissues, including skin, characteristically show uniformity between cells. For this reason, one should expect measurements of normal cell nuclei to also show little variability. This can be illustrated with a histogram of the measurements

Table 1. Group means and *P*s for quantitative biomarkers derived from histochemical staining and image analysis

Parameter	Group			*P*		
	Nonexposed (n = 32)	Sun-damaged (n = 102)	AK (n = 102)	Sun-damaged versus nonexposed	AK versus nonexposed	AK versus sun-damaged
Absorbance	66.9 ± 12.66	71.8 ± 18.90	86.8 ± 27.10	0.5724	<0.0001	<0.0001
Nuclear shape	15.3 ± 0.97	15.5 ± 0.89	17.0 ± 1.68	0.5724	<0.0001	<0.0001
Nuclear size	43.6 ± 6.14	47.8 ± 10.63	60.8 ± 15.49	0.3767	<0.0001	<0.0001
Variability of absorbance	19.7 ± 8.54	22.4 ± 7.70	33.3 ± 11.36	0.3487	<0.0001	<0.0001
Variability of nuclear shape	3.2 ± 2.49	3.2 ± 1.74	5.8 ± 3.47	0.6511	<0.0001	<0.0001
Variability of nuclear size	9.7 ± 3.18	10.8 ± 4.09	17.0 ± 5.52	0.5045	<0.0001	<0.0001
AgNOr no. per nucleus	1.2 ± 0.35	1.0 ± 0.58	1.5 ± 0.43	0.1622	0.0263	<0.0001
Total AgNOr area per nucleus	2.8 ± 1.38	2.64 ± 2.13	5.6 ± 2.89	0.5724	<0.0001	<0.0001
% Ki67	10.5 ± 4.43	16.7 ± 7.60	27.7 ± 9.86	0.0002	<0.0001	<0.0001
% p53	7.8 ± 8.74	19.7 ± 11.82	35.5 ± 10.76	<0.0001	<0.0001	<0.0001

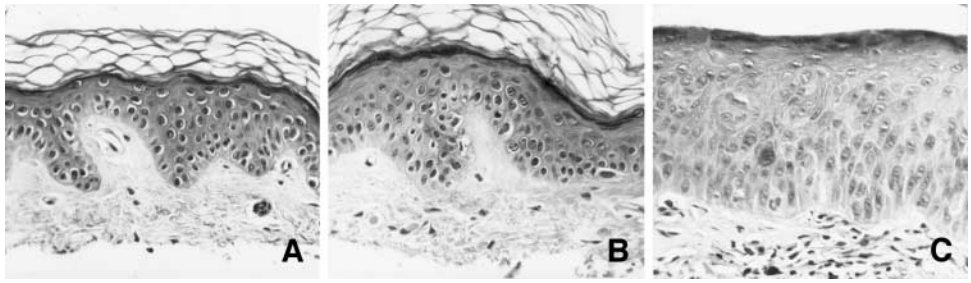

Figure 1. Images of normal skin, sun-damaged skin, and actinic keratosis from the same patient. **A.** Nuclei of normal skin are uniform in size, shape, and staining properties. **B.** Sun-damaged skin shows a mildly thicker epidermis and an increase in dermal elastosis, but the nuclear features are only mildly abnormal. **C.** In contrast, nuclei of AK are markedly more abnormal than those of normal and sun-damaged skin. H&E. original magnification ×100.

(e.g., the absorbance) as shown in Fig. 2A. This histogram shows the distribution of the absorbance of the nuclei for the specimen in Fig. 1A. As expected, the distribution was rather narrow, and the SD of that distribution was small. The average of these SDs between all the specimens of normal skin provides a measure of variability, and this value is listed in the fourth row of Table 1. The normal distributions of the absorbances of a sun-damaged specimen and of an AK are shown in Fig. 2B and C, respectively. Because the AK whose measurements made up the histogram has considerably more variation between cells, the SD of absorbances for that particular specimen was greater. This variability is characteristic of the AKs in our study, and this can be seen in the greater average value for variability in the absorbance of AKs. The variability values of nuclear size and shape were also greater for AKs, as shown in rows 5 and 6 in Table 1.

Image Analysis of Proliferation Markers and p53 Expression. The AgNOr staining patterns of normal, sun-damaged, and AK epidermal nuclei are shown in Fig. 3A, B, and C, respectively. The average AgNOr number per nucleus and average AgNOr area per nucleus were greater in AK than in normal and sun-damaged skin and the average values for each are listed respectively in rows 7 and 8 of Table 1. The AgNOr number and areas were even slightly higher in normal skin than in sun-damaged skin, but the values were still very close to one another. For this reason, it is more likely that the values of AgNOr number and area for normal and sun-damaged skin are essentially the same; but in AK, the values are still greater than either.

The Ki-67 staining patterns of normal, sun-damaged, and AK epidermal nuclei are shown in Fig. 4A, B, and C, respectively. The percentage of cells that are stained is listed for each in row 9 of Table 1. The values reflect the proliferative fraction of cells, which increased as the cells progressed toward sun-damaged and AK. The differences among normal skin, sun-damaged skin, and AK were all significant.

In normal epidermis, p53 is absent or present in only a few cells (Fig. 5A); but in sun-damaged skin (Fig. 5B) and AK (Fig. 5C), many p53-stained cells were seen. The antibody used in this study does not distinguish between mutant and wild-type p53; thus, it is not possible to determine whether the increased p53 expression was due to mutations in the *p53* gene. In many of the AKs, p53 staining seemed in clusters. This clustered

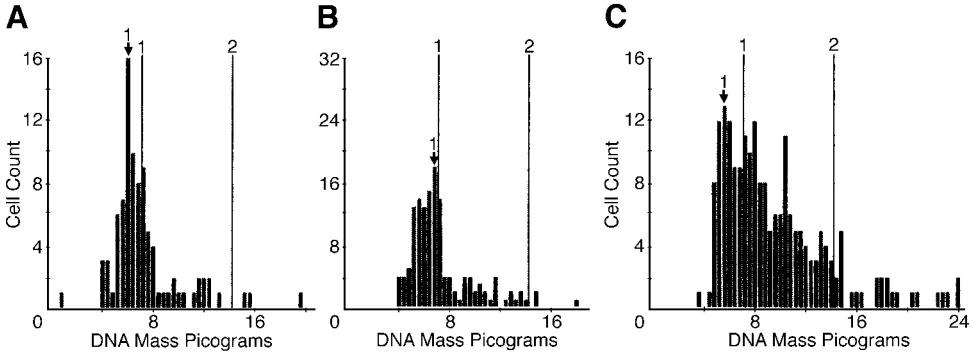

Figure 2. Histograms of absorbances derived from image analysis of Feulgen-stained sections of the biopsies depicted in Fig. 1. The vertical line designated ''1'' represents the absorbance of a diploid nucleus. The absorbance values of individual nuclei in one case each of normal (**A**) and sun-damaged (**B**) skin fall in a narrow distribution around the diploid mean. This smaller distribution is numerically represented by relatively smaller and similar SDs of absorbance (29.82 and 22.11 for the normal and sun-damaged skin biopsies, respectively). The wider range of absorbances of individual nuclei in the case of the AK (**C**) results in a greater value SD of 34.75. The average values of the SD of individual cases provide the data listed in Table 1.

appearance of p53 staining has been previously observed in AK and attributed to clonal proliferations of keratinocytes bearing p53 mutations (21, 23, 24). The percentage of cells that were stained is listed for each in row 10 of Table 1. As in the other parameters that have been measured in this study, AK specimens showed a significantly greater value than both normal and sun-damaged skin. In contrast to the nuclear morphometric parameters, there was a significant increase in the number of cells stained on average in sun-damaged skin in comparison to normal skin.

Discussion

Using computer-assisted image analysis, we have examined the nuclear morphometric parameters of absorbance, nuclear shape, and nuclear size, as well as the variability of these measurements, expressed as the SDs of absorbance, nuclear shape, and nuclear size. For all of the above parameters, normal and sun-damaged skin had similar values, whereas the values for AK were significantly greater. Similarly, the proliferation markers AgNOr number, AgNOr area, and Ki67 staining were greater in AK than in normal and sun-damaged skin. Because the differences in AgNOr number were very small, this marker seems less likely to be clinically useful than AgNOr area or Ki67 staining index. In contrast to AgNOr number and area, Ki67 staining had significantly greater values and thus was a more sensitive measurement of the differences in the proliferative fractions between normal and sun-damaged skin. The fraction of cells staining for p53 also increased as the lesions progressed, with the difference between normal and sun-damage showing significance, indicating that among the parameters we measured, changes in both proliferation and p53 expression as measured in this study seemed earliest in the progression toward AK.

Our results confirm those of previous studies, which have shown increased p53 abnormalities and cellular proliferation in the progression of changes of sun damage to AK (4, 16-24) and an increase in the nuclear morphometric abnormalities that occur in AK and SCC *in situ* in comparison with normal skin (34-39). As in a recent study (38), we have defined the nuclear morphometric characteristics of AK by examining sun-protected skin as well as sun-damaged skin and AK. As in that study, we noted a progressive increase in nuclear morphometric measurements as skin lesions evolved from normal to sun-damaged to AK. In our study, the differences between normal and sun-damaged skin were slight and not statistically significant, but it is possible that a larger sample size might have provided statistical significance. By measuring the variability of nuclear morphometric parameters, we were able to use image analysis to document the nuclear pleomorphism typically seen in AK. This investigation extends previous work by investigating p53, proliferation, and nuclear abnormalities in the same set of samples as those used for nuclear morphometry; thus, our findings provide an examination of the relationship of these parameters in the progression of sun-associated neoplasia.

This study provides quantitative data which illustrates the biology of the progression of sun-induced transformation in the skin. As noted in earlier studies (20-24),

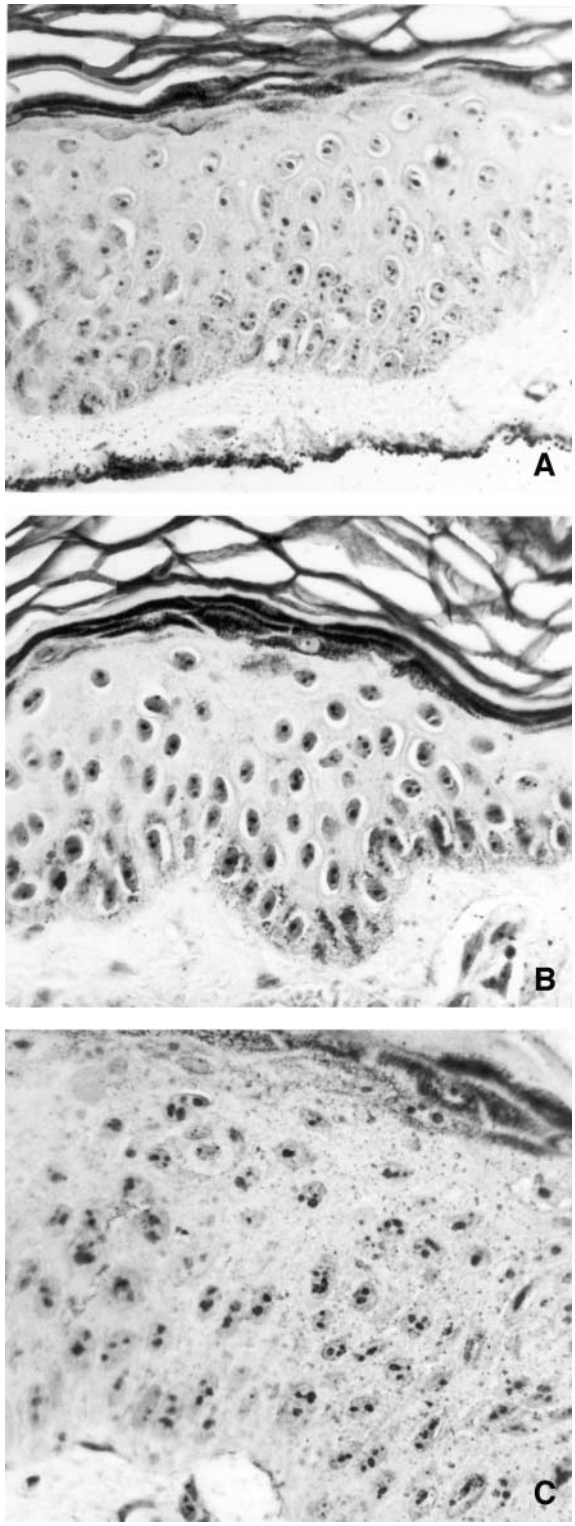

Figure 3. The AgNOr staining patterns of normal (**A**), sun-damaged (**B**), and AK (**C**) epidermal nuclei of the biopsies from Fig. 1. Average AgNOr number per nucleus and average AgNOr area per nucleus were greater in AK than in normal and sun-damaged skin. Original magnification ×160.

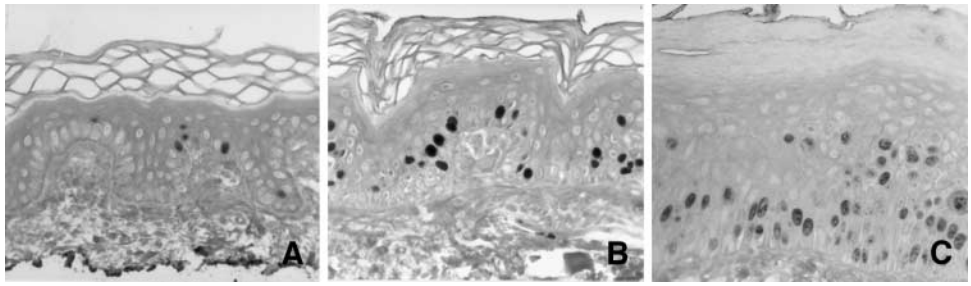

Figure 4. The Ki67 staining patterns of normal, sun-damaged, and AK epidermal nuclei of the biopsies from Fig. 1. **A.** Normal skin shows only a few positively staining basilar nuclei, reflecting a proliferative fraction of 11.6% in this biopsy. **B.** The positively staining proliferative nuclei of sun-damaged epidermis are increased in number (24.8%) relative to normal, but are still primarily in the basal layer. **C.** The average number of staining nuclei is greater in AK at 29.3%, and staining is present within all levels of the epidermis. Immunoperoxidase with methyl green eosin counterstain. Original magnification ×100.

abnormalities of p53, including both over expression of wild-type p53 and mutation, occur soon after sun damage has begun, although AK development is not apparent. Our demonstration that the percentage of p53 over expressing cells further increased in AK is consistent with previous reports of increased p53 expression and mutation in AK (4, 16-19). The nuclear morphometric features, however, did not become significantly abnormal until after p53 abnormalities were detected and when AK was apparent by clinical and histopathological criteria. The proposed role of p53 in protecting cells from DNA damage (16) provides a possible explanation for this observation. According to this view, p53 prevents proliferation of cells with damaged DNA, but since this may not happen in cells with mutated p53, cells with DNA damage will proliferate and accumulate DNA alterations leading to genomic instability. Genomic instability, characterized by abnormal amounts of DNA per cell, and abnormalities of DNA and chromosomal structure or organization have been associated with alterations in nuclear absorbance, shape, size, and variability (31, 32, 45, 46). Thus, our observation that p53 over expression precedes nuclear morphometric abnormalities in the progression of cutaneous squamous cell carcinogenesis suggests that alterations of the *p53* gene precede genomic instability. Further support for this hypothesis might include future *in vitro* studies in which keratinocytes transfected with mutant *p53* are subjected to nuclear morphometric analysis over sequential generations. When considering biomarkers for chemoprevention studies, our data provide a rationale for measuring p53 over expression in a premalignant lesion to predict its susceptibility to develop genomic instability.

Finally, our study illustrates the utility of image analysis in the assessment of chemoprevention and therapeutic agents. Although the features of increased nuclear hyperchromasia, irregularity, area, and variability are well known in AK (2), these variables are not quantifiable by simply viewing histopathologic sections. Image analysis allows for a quantitative value to be determined for these nuclear abnormalities. The degree of reversal of the transformed phenotype can be measured for an agent, and there can be more precise statistical analysis between treatment and placebo groups. Similarly, quantitative values of proliferation by Ki67 immunohistochemistry and AgNOr staining can help determine if an agent affects the proliferation rate of a premalignant lesion. Finally, quantitation of p53 immunostaining can provide a measure of p53 over expression. Although a correlation between p53 expression and mutation is not perfect, clustering of p53 positive nuclei in AK has been reported as evidence of clonal expansion of a keratinocyte bearing a p53 mutation (refs. 21, 23, 24; Fig. 5B and C). Furthermore, an observation of decreased p53 immunostaining after an intervention may have prognostic significance and might provide evidence of a therapeutic effect.

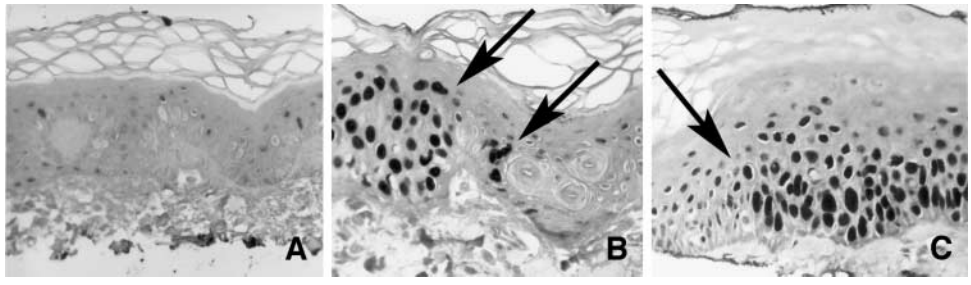

Figure 5. The p53 staining patterns of normal (**A**), sun-damaged (**B**), and AK (**C**) epidermal nuclei of the biopsies from Fig. 1. The average number of staining nuclei is greater in sun-damaged skin than in normal skin, and greater still in AK. In sun-damaged skin and AK, clusters of cells with particularly intense staining (*arrows*) likely represent clonal proliferations of cells harboring p53 mutations. Immunoperoxidase with methyl green eosin counterstain. Original magnification ×100.

Acknowledgments

We thank the Project Officer of the study, Jaye Viner, MD, MPH, of the Division of Cancer Prevention of the National Cancer Institute; our Clinical Coordinator, Sharon Maxwell; Lee Sutherland for providing assistance with image analysis; and Tracey Kingsley for doing the immunoperoxidase reactions.

References

1. Cockerell CJ. Histopathology of incipient intraepidermal squamous cell carcinoma (''actinic keratosis''). J Am Acad Dermatol 2000;42:11–7.
2. Lever WF, Schaumburg-Lever G. Tumors and cysts of the epidermis. In: Lever WF, Schaumburg-Lever G, editors. Histopathology of the skin. 7th ed. Philadelphia: Lippincott; 1990 p. 523–77.
3. Ortonne JP. From actinic keratosis to squamous cell carcinoma. Br J Dermatol 2002;146 Suppl. 61:20–3.
4. Rehman I, Takata M, Wu Y-Y, Rees JL. Genetic change in actinic keratosis. Oncogene 1996;12:2483–90.
5. McNutt NS, Saenz-Santamaria C, Volkenandt M, Shea CR, Albino AP. Abnormalities of p53 protein expression in cutaneous disorders. Arch Dermatol 1994;130:225–32.
6. Basset-Seguin N, Moles JP, Mils V, Dereure O, Guilhou JJ. TP53 tumor suppressor gene and skin carcinogenesis. J Invest Dermatol 1994;103:102–6S.
7. Bito T, Ueda M, Ahmed NU, Nagano T, Ichihashi M. Cyclin D and retinoblastoma gene product expression in actinic keratosis and cutaneous squamous cell carcinoma in relation to p53 expression. J Cutan Pathol 1995;22:427–34.
8. Lu S, Tiekso J, Hietanen S, Syrjanen K, Havu VK, Syrjanen S. Expression of cell-cycle proteins p53, p21 (WAF-1), PCNA and Ki-67 in benign, premalignant and malignant skin lesions with implicated HPV involvement. Acta Derm Venereol 1999;79:268–73.
9. Tucci MG, Offidani A, Lucarini G, et al. Advances in the understanding of malignant transformation of keratinocytes: an immunohistochemical study. J Eur Acad Dermatol Venereol 1998;10:118–24.
10. Bartek J, Bartkova J, Vojtesek B, et al. Aberrant expression of the p53 oncoprotein is a common feature of a wide spectrum of human malignancies. Oncogene 1991;6:1699–703.
11. Nigro JM, Baker SJ, Preisinger AC, et al. Mutations in the p53 gene occur in diverse human tumour types. Nature 1989;342:705–8.
12. Vousden KH. P53: death star. Cell 2000;103:691–4.
13. Brash DE, Ponten J. Skin precancer. Cancer Surv 1998;32:69–113.
14. Ouhit A, Muller HK, Davis DW, Ullrich SE, McConkey D, Ananthaswamy HN. Temporal events in skin injury and the early adaptive responses in ultraviolet-irradiated mouse skin. Am J Pathol 2000;156:201–7.
15. Healy E, Reynolds NJ, Smith MD, Campbell C, Farr PM, Rees JL. Dissociation of erythema and p53 protein expression in human skin following UVB irradiation, and induction of p53 protein and mRNA following application of skin irritants. J Invest Dermatol 1994;103:493–9.
16. Ziegler A, Jonason AS, Leffell DJ, et al. Sunburn and p53 in the onset of skin cancer. Nature 1994;372:773–6.
17. Nelson MA, Einspahr JG, Alberts DS, et al. Analysis of the p53 gene in human precancerous actinic keratosis lesions and squamous cell cancers. Cancer Lett 1994;85:23–9.
18. Campbell C, Quinn AG, Ro YS, Angus B, Rees JL. p53 mutations are common and early events that precede tumor invasion in squamous cell neoplasia of the skin. J Invest Dermatol 1993;100:746–8.
19. Einspahr JG, Nelson MA, Saboda K, Warneke J, Bowden GT, Alberts DS. Modulation of biologic endpoints by topical difluoromethylornithine (DFMO), in subjects at high-risk for nonmelanoma skin cancer. Clin Cancer Res 2002;8:149–55.
20. Einspahr J, Alberts DS, Aickin M, et al. Expression of p53 protein in actinic keratosis, adjacent, normal-appearing, and non-sun-exposed human skin. Cancer Epidemiol Biomarkers Prev 1997;6:583–7.
21. Jonason AS, Kunala S, Price GJ, et al. Frequent clones of p53-mutated keratinocytes in normal human skin. Proc Natl Acad Sci U S A 1996;93:14025–9.
22. Nakazawa H, English D, Randell PL, et al. UV and skin cancer: specific p53 gene mutation in normal skin as a biologically relevant exposure measurement. Proc Natl Acad Sci USA 1994;91:360–4.
23. Tabata H, Nagano T, Ray AJ, Flanagan N, Birch-MacHin MA, Rees JL. Low frequency of genetic change in p53 immunopositive clones in human epidermis. J Invest Dermatol 1999;113:972–6.
24. Ren ZP, Hedrum A, Ponten F, et al. Human epidermal cancer and accompanying precursors have identical p53 mutations different from p53 mutations in adjacent areas of clonally expanded non-neoplastic keratinocytes. Oncogene 1996;12:765–73.
25. Jiang W, Ananthaswamy HN, Muller HK, Kripke ML. p53 protects against skin cancer induction by UV-B radiation. Oncogene 1999;18:4247–53.
26. Marks R, Rennie G, Selwood TS. Malignant transformation of solar keratoses to squamous cell carcinoma. Lancet 1988;1:795–7.
27. Einspahr JG, Alberts DS, Warneke JA, et al. Relationship of p53 mutations to epidermal cell proliferation and apoptosis in human UV-induced skin carcinogenesis. Neoplasia 1999;1:468–75.
28. Alberts DS, Dorr RT, Einspahr JG, et al. Chemoprevention of human actinic keratoses by topical 2-(difluoromethyl)-DL-ornithine. Cancer Epidemiol Biomark Prev 2000;9:1281–6.
29. Dore JF, Pedeux R, Boniol M, Chignol MC, Autier P. Intermediate-effect biomarkers in prevention of skin cancer. I.A.R.C. Sci Publ 2001;154:81–91.
30. Boone CW, Kelloff GJ. Biomarker end-points in cancer chemoprevention trials. IARC Sci Publ 1997;142:273–80.
31. Cohen C. Image cytometric analysis in pathology. Hum Pathol 1996;27:482–93.
32. Millot C, Dufer J. Clinical applications of image cytometry to human tumour analysis. Histol Histopathol 2000 15:1185–200.
33. True LD. Morphometric applications in anatomic pathology. Hum Pathol 1996;27:450–67.
34. Bozzo PD, Vaught LC, Alberts DS, Thompson D, Bartels PH. Nuclear morphometry of solar keratosis. Anal Quant Cytol Histol 1998;20:21–8.
35. Biesterfeld S, Pennings K, Grussendorf-Conen EI, Bocking A. Aneuploidy in actinic keratosis and Bowen's disease-increased risk for invasive squamous cell carcinoma? Br J Dermatol 1995;133:557–60.
36. Narvaez D, Kanitakis J, Euvrard S, Schmitt D, Faure M, Claudy A. Comparative nuclear morphometric analysis of aggressive and non-aggressive squamous cell carcinomas of the skin. Acta Derm Venereol 1997;77:115–7.
37. Newton JA, Camplejohn RS, McGibbon DH. Aneuploidy in Bowen's disease. Br J Dermatol 1986;114:691–4.
38. Ranger-Moore J, Bozzo P, Alberts D, et al. Karyometry of nuclei from actinic keratosis and squamous cell cancer of the skin. Anal Quant Cytol Histol 2003;25:353–61.
39. Bozzo P, Alberts DS, Vaught L, et al. Measurement of chemopreventive efficacy in skin biopsies. Anal Quant Cytol Histol 2001;23:300–12.
40. Linden KG, Carpenter PM, McLaren CE, et al. Chemoprevention of nonmelanoma skin cancer: experience with a polyphenol from green tea. In: Senn H-J, Morant R, editors. Recent results in cancer research. Vol. 163. Berlin: Springer-Verlag; 2003. p. 165–71.
41. Ploton D, Menager M, Jeannesson P, Himber G, Pigeon F, Adnett JJ. Improvement in the staining in the visualization of the argyrophilic proteins of the nucleolar organizer region at the optical level. Histochem J 1986;18:5–14.
42. Bacus JW, Grace LJ. Optical microscope system for standardized cell measurements and analyses. Appl Optics 1987;26:3280–93.
43. Box GPE, Cox DR. An analysis of transformations. J R Stat Soc 1964;26:211–43.
44. Westfall PH, Young SS. Resampling-based multiple testing: examples and methods for *P*-value adjustment. New York: John Wiley & Sons; 1993.
45. Gisselsson D, Bjork J, Hoglund M, et al. Abnormal nuclear shape in solid tumors reflects mitotic instability. Am J Pathol 2001;158:199–206.
46. Mulder JW, Offerhaus GJ, de Feyter EP, et al. The relationship of quantitative nuclear morphology to molecular genetic alterations in the adenoma-carcinoma sequence of the large bowel. Am J Pathol 1992;141:797–804.